communications
earth & environment

ARTICLE

https://doi.org/10.1038/s43247-021-00187-7 OPEN

Exogenous copper sulfide in returned asteroid Itokawa regolith grains are likely relicts of prior impacting body

Katherine D. Burgess [1✉] & Rhonda M. Stroud [1]

Samples from asteroid 25143 Itokawa returned by the Hayabusa mission have been identified as LL4-6 ordinary chondrite materials and have shown it to be a rubble pile that aggregated after break-up of a parent body. Here we investigate particle RB-CV-0038 from the Itokawa regolith using scanning and transmission electron microscopy and energy dispersive spectroscopy. We identify a cubanite-chalcopyrite-troilite-pyrrhotite assemblage, the phases and structure of which are indicative of low-temperature, aqueous alteration. Cubanite is stable only at temperatures below around 250 °C and has thus far only been identified in CI carbonaceous chondrites and the comet 81P/Wild2 sample suite. Chalcopyrite is also very rare in the meteorite record and is found mostly in R chondrites and some CK chondrites. Because the Itokawa parent body experienced significant thermal alteration with little evidence of low-temperature equilibration or aqueous alteration, we propose that the assemblage we identify is most likely exogenous and represents a component of an impacting body.

[1] U.S. Naval Research Laboratory, Washington, DC, USA. ✉email: kate.burgess@nrl.navy.mil

The samples returned from asteroid 25143 Itokawa by the Hayabusa spacecraft have provided a significant amount of new information about asteroids in general and S-type asteroids specifically[1]. The mineral and glass phases present and their compositions provide fundamental constraints on how the Itokawa parent body formed and evolved. Observations show that Itokawa is a rubble pile that aggregated after the break-up of the parent body (possibly multiple times)[2]. Many of the particles from Itokawa have angular edges, indicating they are fragments of grains from mechanical crushing, while the rounded edges of some particles are likely due to subsequent mechanical abrasion[3,4]. Evidence of small micrometeorite impacts and microbreccia formation has been noted on a number of Itokawa grains[5–7], but thus far, no clear remnants of potential impactors have been identified. Other rubble pile asteroids, (101955) Bennu and (162172) Ryugu, have recently been shown to contain significant amounts of exogenous material, recognizable using remote sensing spectra[8,9], but no such signals have been reported for Itokawa. However, small adhered Cu-sulfide grains observed previously on a particle could represent exogenous material[6].

Sulfide assemblages, with or without metal, have been used in a number of meteorite studies to determine conditions on parent body asteroids for both primary and alteration phases[10–17]. The Fe-Ni-sulfides troilite, pyrrhotite, and pentlandite are common on both ordinary and carbonaceous chondrites and can record oxygen and sulfur fugacity, temperature, pH, and shock conditions throughout their history. Other less common sulfide phases, such as chalcopyrite ($CuFeS_2$), cubanite ($CuFe_2S_3$), and sphalerite ((Zn,Fe)S) can provide additional constraints on alteration conditions[14]. The Cu-bearing sulfide phases specifically are reported in only a few types of meteorites[18,19], indicating a limited range of conditions under which these materials form on planetary bodies. The presence of sulfide phases that record low-temperature conditions within the partially to fully equilibrated samples from Itokawa provide evidence of the presence of microxenoliths from other bodies and thus clues to interactions that occurred on Itokawa.

We present data from Itokawa particle RB-CV-0038 showing it contains a cubanite-chalcopyrite-pyrrhotite-troilite assemblage consistent with low-temperature aqueous alteration. Such an assemblage is inconsistent with the thermal metamorphism experienced by the Itokawa parent body and therefore the material must have become part of Itokawa after thermal alteration. We conclude that this grain, and the other Cu-sulfides noted on Itokawa, likely originated in a primitive, hydrated asteroid source such as a CI chondrite-like parent body or D- or P-type asteroids, which have been proposed as the source of other unique meteorites and microxenoliths that experienced low-temperature aqueous alteration[20,21].

Results

Troilite, pyrrhotite, and olivine (Fo_{72}) are the dominant phases in RB-CV-0038 (hereafter, C0038), with minor plagioclase or glass present either as part of the grain or as adhered particles (Fig. 1; Supplementary Table 1). A ~2 μm Cu-Fe-sulfide grain is present with the Fe-sulfide at the interface with the olivine. The surface of the olivine has many sub-micron adhered grains but no clear impact-related features. Adhered grains captured by the FIB sections are also olivine and of similar composition to the larger grain. There is a large conchoidal fracture on the olivine, as well as some wavy and stepped surfaces[3], and the scanning transmission electron microscopy (STEM) data show a lack of any distinct space weathering rim. There is also no evidence of a space weathering rim at the grain boundary between the olivine and iron sulfide. The boundary between them is smooth, and there is a distinct step up on the olivine next to the sulfide. The surface of the Fe-sulfide is highly varied, with some portions having a smooth, almost flow-like texture while other regions are fractured (wavy and stepped) or have sharp facets somewhat similar to the concentric stepped surfaces noted on other Itokawa particles[3].

Within the sulfide portion of the grain, there are several different Fe-sulfide grains in addition to the Cu-Fe-sulfide grain (Fig. 2). The Cu-Fe-sulfide grain contains cubanite (cb; $CuFe_2S_3$) and possibly monoclinic 4C-pyrrhotite (4C-po; Fe_7S_8) as evidenced by selected area electron diffraction (SAED) patterns. The pattern in Fig. 2c cannot be matched by the basic unit cell of cubanite ($a = 6.463$, $b = 11.117$, $c = 6.234$;[22]); some reflections can best be indexed assuming a superstructure with a tripling of c. A better fit to about one-quarter of the collected patterns from the cubanite grain is made by adjusting a slightly to be more similar to b of 4C-pyrrhotite (=6.850 [23]), which could indicate significant strain due to the presence of oxygen in the lattice or incomplete replacement of pyrrhotite by cubanite during the reaction. Most reflections in other SAED patterns from the Cu-Fe-sulfide grain are consistent with the identification of cubanite and pyrrhotite, with remaining reflections not easily matched to any expected phase and likely indicating deformation (Supplementary Fig. 1). Isocubanite, which has the same composition as cubanite, is not seen. Rings consistent with magnetite are also seen in some SAED patterns from the cubanite, but this is likely an artifact from FIB preparation. However, magnetite is present elsewhere in the sample, and described in detail below. Electron energy-loss spectroscopy (EELS) Fe and Cu L-edge data are unable to distinguish between cubanite and chalcopyrite (cp) but show clear differences from other Cu-sulfide phases, such as bornite (Cu_5FeS_4) and covellite (CuS) (Fig. 3).

The Cu content of the Cu-rich sulfide must be estimated due to the Cu system peaks in our STEM energy-dispersive X-ray spectroscopy (EDS) data caused by copper in the microscope pole

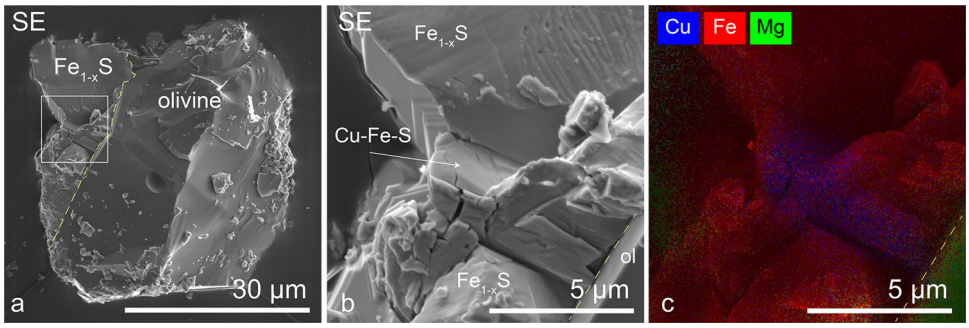

Fig. 1 Images of RB-CV-0038. a Secondary electron (SE) image of C0038. Fe-sulfide is in the top left and the rest of the grain is olivine. **b** SE image showing the Cu-Fe-sulfide grain present with the iron sulfide. **c** EDS map showing the Cu-rich grain. Dotted lines indicate the olivine-sulfide boundary.

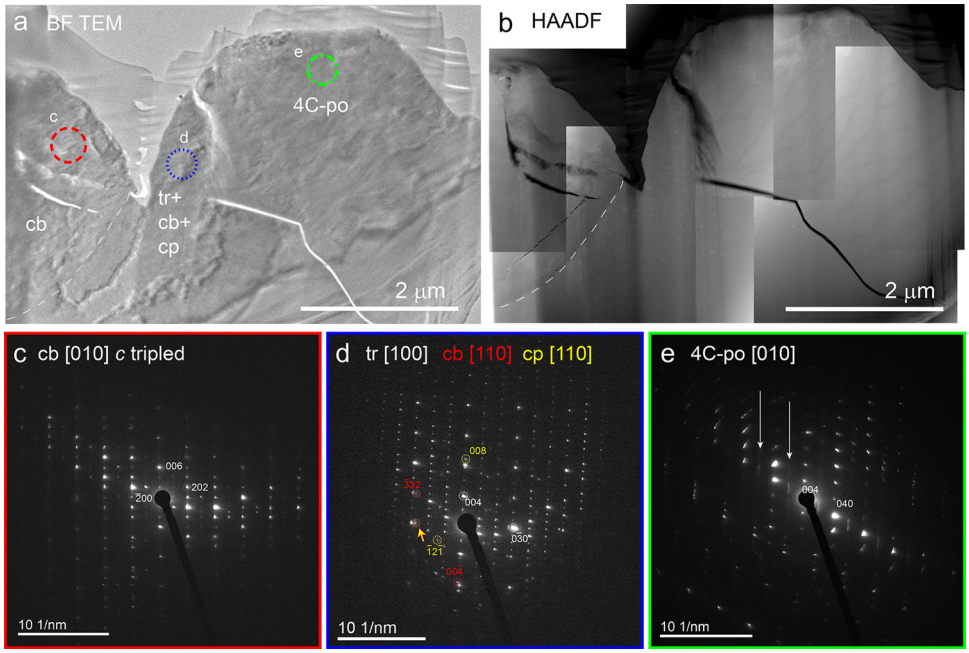

Fig. 2 FIB section and diffraction patterns from particle C0038. a Bright field TEM image and **b** HAADF STEM image mosaic of sulfide grains from C0038. Cubanite (cb) is to the left; troilite (tr) with Cu-rich regions is next to the cubanite; pyrrhotite (4C-po) flame texture is to the right. SAED patterns from **c** cubanite, **d** troilite (tr), with faint chalcopyrite (cp) (yellow) and cubanite (red) reflections, and **e** 4C-pyrrhotite with streaking that could indicate the presence of NC-pyrrhotite.

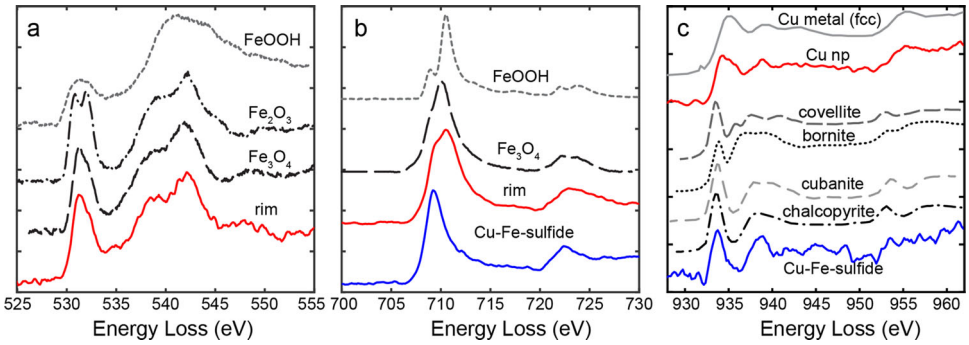

Fig. 3 EELS data from regions in C0038 and standards. a O K-edge, **b** Fe L-edge, and **c** Cu L-edge EELS from various regions in and around the crack in the chalcopyrite grain, showing the crack rim (red) is magnetite, Cu-rich nanoparticles are fcc-Cu metal, and Cu in the sulfide matches both chalcopyrite and cubanite[47,48]. Fe-oxide standards shown for comparison[49].

piece cover and in the sample holder (Supplementary Fig. 4 and Supplementary Table 1). In the Cu-rich phase, Fe/S ~ 0.65–0.73. If we assume all cation sites are filled (i.e., Fe + Cu = S), we find Cu/Fe of 0.55–0.37, consistent with cubanite or isocubanite, possibly mixed with pyrrhotite. There is ~8 at% O measured in the bulk of the Cu-Fe-sulfide as well. However, Fe L-edge EELS shows no evidence of oxidation, and oxygen was not included in the calculations to determine Cu/Fe. Both the Cu-Fe-sulfide and Fe-sulfide in C0038 lack Ni.

The iron-sulfide portion of the particle is defect-rich and contains multiple grains in the section near the Cu-Fe-sulfide (Fig. 2). The grain nearest the Cu-Fe-sulfide has a slightly mottled appearance in high-angle annular dark-field (HAADF) imaging (Fig. 2b), and bright regions 50–60 nm across seen in HAADF images correlate with increased Cu in EDS maps (Fig. 4a, b). The average composition for this portion of the Fe-sulfide has ~2 at% more Cu than the Fe-sulfide further from the cubanite. The mottled grain, like the Cu-Fe-sulfide, contains ~6 at% O with no evidence of oxidation in EELS. The Cu-free sulfide contains O ~3 at% showing some of the O is not from sample preparation and could be from the aqueous alteration (Supplementary Fig. 4). The flame-like texture seen in the grain to the right in Fig. 2 is interpreted as the exsolution of two types of pyrrhotite[12] but is too finely intergrown for any compositional differences to be seen in EDS maps. The average measured Fe/S composition for the grain (x = ~0.09 in $Fe_{1-x}S$) is consistent with a 4C-pyrrhotite or a mixture of 4C and NC-pyrrhotites. In NC-pyrrhotites, NC indicates a variable, non-integral superstructure based on the NiAs-type unit cell where troilite is 2C.

Diffraction patterns were collected from several areas within the Fe-sulfide. Closest to the Cu-rich grain, these patterns show the presence of troilite (tr), with spots consistent with both chalcopyrite and cubanite present in some SAED images (Fig. 2d and Supplementary Fig. 2). In the region with the flame texture, the only clearly indexed phase is 4C-pyrrhotite, although streaking and some excess reflections could indicate the presence of NC-pyrrhotite (Fig. 2e and Supplementary Fig. 3). Some diffraction patterns did not index fully to these phases, and there is evidence of deformation and a large number of defects.

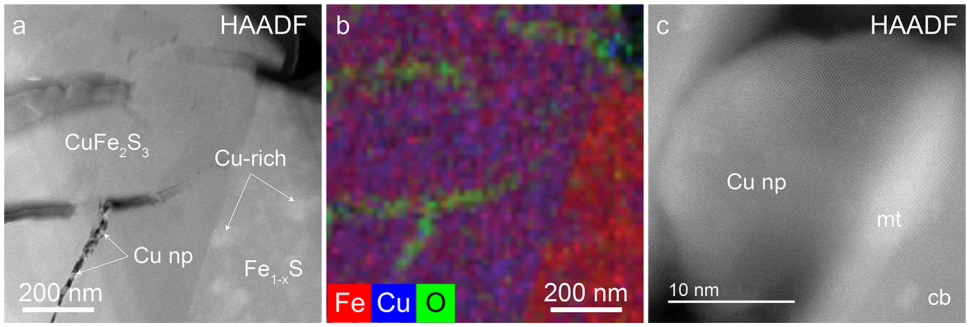

Fig. 4 Images of a crack in cubanite in C0038. a HAADF and **b** semi-quantitative EDS map of cubanite and mottled troilite in a FIB section from C0038. The crack in Cu-rich phase has oxidized, Cu-free magnetite edges and is filled with Cu metal nanoparticles. The Cu enrichment of the bright spots in the Fe-sulfide can also be seen. **c** HAADF image of Cu nanoparticle and brighter magnetite (mt) rim of a crack in cubanite (cb).

Several cracks are present in the Cu-Fe-sulfide, one of which is perpendicular to the FIB section. The crack has oxidized Fe-rich edges and is decorated by Cu metal nanoparticles (Fig. 4). No other material (e.g., silica) is present in the crack. The edges of the crack are sulfur-free to 5 nm and have been oxidized to magnetite as indicated by both EELS (Fig. 3) and lattice spacings in high-resolution images. It is unclear if the other O-rich regions in the Cu-Fe-sulfide grain are similar cracks with oxidized edges that were oblique to the section as thinned or if the excess O is an artifact of the FIB preparation.

Discussion

The sulfide grains in Itokawa particle RB-CV-0038 are inconsistent with the primary formation on the Itokawa parent body, and must instead be a microxenolith of carbonaceous chondrite or cometary origin. Cubanite and 4C-pyrrhotite together, which has been identified in CI chondrites, indicate temperatures less than 200 °C[14]. By contrast, LL6 particles among the Itokawa sample set equilibrated at temperatures of ~800 °C with slow cooling to only ~600 °C[1,24]. The mottled troilite–cubanite–chalcopyrite grain with low amounts of copper present between the cubanite and 4C-pyrrhotite suggests the interaction of the pyrrhotite with a Cu-bearing fluid during low-temperature aqueous alteration to form the cubanite[25,26]. Structural and petrologic evidence from CI chondrites show the cubanite in those meteorites formed at a later stage than the pyrrhotite as well[10,14].

Cubanite, a Cu-Fe-sulfide, is known only in terrestrial ore deposits, comet 81P/Wild2, and CI-chondrite materials[14,27]. Cubanite goes through an irreversible transformation to isocubanite at 200–250 °C depending on heating rate[28]. Isocubanite is not stable at low temperature (below ~250 °C) and decomposes upon slow cooling to pyrrhotite and chalcopyrite[28,29]. Experimental work at conditions relevant to the CI-chondrite parent body (150–200 °C; pH 9–10) show the presence of cubanite in runs with both metal and sulfide starting materials, and chalcopyrite was identified by XRD in all of the experimental runs[30]. The experimental grains analyzed for structural details showed doubling or quadrupling of *a* and *c* to form superstructures in different grains[30], while no superstructures were noted in the natural Wild 2 or Orguiel cubanites[14]. This is in contrast to our measured tripling of *c* and indicates likely differences in formation and/or alteration histories[30]. In addition to the low-temperature formation of the cubanite, monoclinic 4C-pyrrhotite is stable at temperatures <250 °C and has been identified with cubanite in CI chondrites[14]. Exsolution of NC-pyrrhotite in 4C-pyrrhotite is common in terrestrial samples[17].

Low-temperature aqueous alteration did occur on ordinary chondrite parent bodies, as evidenced by bleached chondrules in ordinary chondrites of all metamorphic grades[31]. However, thermal metamorphism occurred after most of the aqueous alteration, and for our grain, would have removed the low-temperature exsolution features. The reported presence of NaCl on at least several different Itokawa grains[32,33] could indicate later, localized aqueous processing that may also have affected the oxidized crack in the cubanite. However, it is unclear if the NaCl grains are from the asteroid or are due to terrestrial contamination[33]. Magnetite, as seen on the crack rim, forms under high pH (8–11), low-temperature conditions on chalcopyrite[34,35]. Similar reactions likely would take place for the oxidation of cubanite surfaces and provide constraints on temperature and fluid composition during alteration. Iron sulfates are formed during reactions at low pH while copper oxidation products were also present in non-aqueous (air) experiments[35].

Copper on LL chondrites is found in Fe-Ni metal and as native Cu[36], and a localized shock event could lead to the mixing of Cu metal with iron-sulfide to form a Cu-Fe-sulfide. This is the likely formation mechanism of a bornite-like phase reported with troilite and native Cu in the Pultusk meteorite (H4-6)[37]. Above 600 °C, sulfide of the composition measured here (~$CuFe_2S_3$) is within the range of a cubic intermediate solid solution (*iss*) that at high temperature falls between the bornite solid solution and the pyrrhotite solid solution[38]. Upon cooling, chalcopyrite can exsolve within the isocubanite matrix[39], but cubanite does not form[28]. This cubic *iss* is likely the same phase identified in a number of stony meteorites as chalcopyrrhotite[40] and is structurally the same as isocubanite[39].

Particle C0038 was likely once part of a larger breccia that fused the exogenous sulfide portion to olivine from the Itokawa parent body, possibly prior to the formation of Itokawa itself. The aqueous alteration event that caused the oxidation of the crack in the cubanite could also have led to its fusing with the olivine. The composition of the olivine in C0038 falls within the expected range for LL chondrite material and is closely related to phases previously measured in Itokawa particles, suggesting that the microxenolith comprises only a portion of the particle. The olivine composition is less magnesian than typical for CI chondrites ($Fa_{0.5–26}$ in Orgueil[41] compared to Fa_{29} here), and there is no evidence of any alteration within the olivine itself or along the boundary between the sulfide assemblage and the olivine.

Microxenoliths of carbonaceous chondrite material have been identified in ordinary chondrites[42], and CI-like material specifically has been found in several meteorites[43]. However, this grain has several clear differences from the cubanite identified in CI chondrites. In Orgueil, veins in two different cubanite grains have Ni-bearing layers[14], but we observed no Ni in the crack in the cubanite or in the adjacent pyrrhotite. However, it is possible that pentlandite was previously associated with the sulfide grains and was broken off during the impact that brought it to Itokawa or by

subsequent abrasion. In addition to the different cubanite superstructure between this grain and those previously reported[14,30], troilite has not been identified with the cubanite in CI chondrites[14], and its presence could indicate different conditions than seen on the CI parent body. However, clasts in CI chondrites have been shown to have heterogeneous degrees of alteration[44], and thus it is possible this grain is from a location that was altered under different conditions than those identified in the meteorite collection. It is also possible the grain is from another parent body that experienced many of the same conditions necessary for cubanite formation. Ultra-primitive D- and P-type asteroids have been proposed as parent bodies for Tagish Lake meteorite[20] and a primitive organic-rich clast recently reported in Zag (H3-6) meteorite[21]. Both of these samples experienced low-temperature aqueous alteration possibly consistent with cubanite formation, and both contain locally abundant sulfides, although a Cu-bearing phase has not been reported. Pyrrhotites in Tagish Lake, as in CIs, are often Ni-rich compared to our grain, although the sulfides exhibit a wide range of alteration textures[45]. Additionally, the cubanite in the Wild2 sample suite may have formed during alteration of the comet[14], which in turn could mean that cometary material is also a possible source for the cubanite on Itokawa, although such alteration is not thought to be pervasive on comets.

Recently, significant amounts of proposed exogenous materials have been identified spectroscopically on asteroids (101955) Bennu[8] and (162172) Ryugu[9]. Exogenous material was not recognized spectrally on Itokawa, but exogenous material containing significant sulfide phases may not necessarily be apparent. Considering the relative rarity of Cu-bearing sulfides in the meteorite record[18], it seems quite possible that the Cu-sulfides noted in a previous Itokawa sample[6] are related to the chalcopyrite identified here. Identification of multiple, possibly related, exogenous grains within the sample set suggests the impact event that mixed the cubanite with the indigenous material was more than a single micrometeoroid, or that interactions with the same body occurred multiple times. While our particle C0038 was located in Room-B, the other particles were from Room-A and collected during a separate touchdown by Hayabusa[46], indicating the exogenous material is more widespread than would be possible from a single micrometeorite or IDP. The presence of exogenous material on Bennu and Ryugu, and now on Itokawa, confirms that asteroids with material on their surface from unrelated parent bodies are the norm rather than an exception.

Methods

Particle RB-CV-0038 (C0038) was provided to NRL as part of the 3rd International Announcement of Opportunity by JAXA. The particle is composed of olivine and sulfide and is ~40 µm across. It was mounted in epoxy such that most of the grain was available for imaging, then coated by 80 nm of evaporated carbon to reduce charging and provide added protection of the surface during the ion beam deposition and milling. Scanning electron microscope (SEM) imaging and focused ion beam (FIB) sample preparation were done using an FEI Helios G3 equipped with an Oxford 150 mm^2 SDD energy dispersive X-ray spectrometer (EDS). After imaging, protective straps of C or Pt were deposited on regions of interest, and multiple sections suitable for scanning electron microscopy (STEM) analysis were extracted from the particle. Final thicknesses, determined using electron energy-loss spectroscopy (EELS), are $t/\lambda < 1$ where t is the sample thickness and λ is the scattering cross-section. Samples were prepared using a 30 kV Ga^+ beam, with final thinning and cleaning of some sections done at a lower voltage (8 or 16 kV). Most samples were mounted on Cu half-grids, but one extracted from a region known to contain Cu (from SEM-EDS) was mounted on a Mo half-grid. STEM analysis was carried out with the Nion UltraSTEM200-X at NRL. The microscope is equipped with a Gatan Enfinium ER spectrometer for EELS and a windowless, 0.7 sr Bruker SDD-EDS detector. Data were collected at 200 kV, 70–90 pA. Selected area electron diffraction (SAED) patterns and bright-field images were collected on a JEOL2200F. SAED patterns were measured based on calibrated camera constants, and phase identifications were compared to simulated patterns from the software program SingleCrystal by CrystalMaker Software Ltd.

Quantification of STEM-EDS data was performed with the Cliff-Lorimer method and detector-specific k-factors obtained calculated with the Bruker Espirit 1.93 software. A system Cu peak is present in all data due to Cu being used in the sample holder and pole piece cover. This peak is significantly reduced by the use of a Mo half-grid to support the FIB section and optimization of the sample position relative to the grid posts and EDS detector, but assumptions about phase stoichiometry must be made to determine the Cu content of a material. We calculate Cu in Cu-bearing phases assuming contribution from system peaks is the same as that in Cu-free pyrrhotite or alternatively by assuming $(Cu+Fe)/S = 1$ and calculating Cu in the sample after measuring Fe and S. We obtain consistent compositions for each calculation method for the cubanite grain, providing validation for our assumptions.

Data availability

The data that support the figures in this article available at https://doi.org/10.13140/RG.2.2.17763.27689

Received: 21 July 2020; Accepted: 13 May 2021;
Published online: 09 June 2021

References

1. Nakamura, T. et al. Itokawa dust particles: a direct link between S-type asteroids and ordinary chondrites. *Science* **333**, 1113–1116 (2011).
2. Fujiwara, A. et al. The rubble-pile asteroid Itokawa as observed by Hayabusa. *Science* **312**, 1330–1334 (2006).
3. Matsumoto, T. et al. Nanomorphology of Itokawa regolith particles: Application to space-weathering processes affecting the Itokawa asteroid. *Geochim. Cosmochim. Acta* **187**, 195–217 (2016).
4. Tsuchiyama, A. et al. Three-dimensional structure of Hayabusa samples: Origin and evolution of Itokawa regolith. *Science* **333**, 1125–1128 (2011).
5. Matsumoto, T., Hasegawa, S., Nakao, S., Sakai, M. & Yurimoto, H. Population characteristics of submicrometer-sized craters on regolith particles from asteroid Itokawa. *Icarus* **303**, 22–33 (2018).
6. Nakamura, E. et al. Space environment of an asteroid preserved on micrograins returned by the Hayabusa spacecraft. *Proc. Nat. Acad. Sci. USA* **109**, E624–E629 (2012).
7. Matsumoto, T., Miyake, A., Harries, D., Noguchi, T. & Langenhorst, F. Shock melting features in regolith particles of S-type asteroid Itokawa. In *Annual Meeting of Meteoritical Society* 6213 (2019).
8. DellaGiustina, D. N. et al. Exogenic basalt on asteroid (101955) Bennu. *Nat. Astron.*, https://doi.org/10.1038/s41550-020-1195-z (2020).
9. Tatsumi, E. et al. Collisional history of Ryugu's parent body from bright surface boulders. *Nat. Astron.* **5**, 39–45 (2020).
10. Bullock, E. S., Gounelle, M., Lauretta, D. S., Grady, M. M. & Russell, S. S. Mineralogy and texture of Fe-Ni sulfides in CI1 chondrites: Clues to the extent of aqueous alteration on the CI1 parent body. *Geochim. Cosmochim. Acta* **69**, 2687–2700 (2005).
11. Singerling, S. A. & Brearley, A. J. Altered primary iron sulfides in CM2 and CR2 carbonaceous chondrites: insights into parent body processes. *Meteor. Planet. Sci.* **55**, 496–523 (2020).
12. Harries, D. & Langenhorst, F. The nanoscale mineralogy of Fe,Ni sulfides in pristine and metamorphosed CM and CM/CI-like chondrites: tapping a petrogenetic record. *Meteor. Planet. Sci.* **48**, 879–903 (2013).
13. Schrader, D. L. & Zega, T. J. Petrographic and compositional indicators of formation and alteration conditions from LL chondrite sulfides. *Geochim. Cosmochim. Acta* **264**, 165–179 (2019).
14. Berger, E. L., Zega, T. J., Keller, L. P. & Lauretta, D. S. Evidence for aqueous activity on comet 81P/Wild 2 from sulfide mineral assemblages in Stardust samples and CI chondrites. *Geochim. Cosmochim. Acta* **75**, 3501–3513 (2011).
15. Brearley, A. J. & Martinez, C. Ubiquitous exsolution of pentlandite and troilite in pyrrhotite from the TIL 91722 CM2 carbonaceous chondrite: a record of low temperature solid state processes. In *Lunar and Planetary Science Conference* 1689 (2010).
16. Rubin, A. E. Magnetite-sulfide chondrules and nodules in CK carbonaceous chondrites: Implications for the timing of CK oxidation. *Meteoritics* **28**, 130–135 (1993).
17. Harries, D. & Zolensky, M. E. Mineralogy of iron sulfides in CM1 and CI1 lithologies of the Kaidun breccia: Records of extreme to intense hydrothermal alteration. *Meteor. Planet. Sci.* **51**, 1096–1109 (2016).
18. Rubin, A. E. Mineralogy of meteorite groups. *Meteor. Planet. Sci.* **32**, 231–247 (1997).
19. Rubin, A. E. & Ma, C. Meteoritic minerals and their origins. *Geochemistry* **77**, 325–385 (2017).

20. Brown, P. G. et al. The fall, recovery, orbit, and composition of the Tagish Lake meteorite: A new type of carbonaceous chondrite. *Science* **290**, 320–325 (2000).
21. Kebukawa, Y. et al. A novel organic-rich meteoritic clast from the outer solar system. *Sci. Rep*. **9**, 3169 (2019).
22. Buerger, M. The crystal structure of cubanite. *Am. Mineral.* **32**, 415–425 (1947).
23. Tokonami, M., Nishiguchi, K. & Morimoto, N. Crystal structure of a monoclinic pyrrhotite (Fe_7S_8). *Am. Mineral.* **57**, 1066–1080 (1972).
24. Harries, D. & Langenhorst, F. Carbide-metal assemblages in a sample returned from asteroid 25143 Itokawa: evidence for methane-rich fluids during metamorphism. *Geochim. Cosmochim. Acta* **222**, 53–73 (2018).
25. Elliot, A. D. & Watling, H. R. Chalcopyrite formation through the metathesis of pyrrhotite with aqueous copper. *Geochim. Cosmochim. Acta* **75**, 2103–2118 (2011).
26. Cowper, M. & Rickard, D. Mechanism of chalcopyrite formation from iron monosulphides in aqueous solutions (<100 °C, pH 2–4.5). *Chem. Geol.* **78**, 325–341 (1989).
27. Kerridge, J. F., Macdougall, J. D. & Marti, K. Clues to the origin of sulfide minerals in CI chondrites. *Earth Planet. Sci. Lett.* **43**, 359–367 (1979).
28. Dutrizac, J. Reactions in cubanite and chalcopyrite. *Canad. Mineral.* **14**, 172–181 (1976).
29. Pruseth, K. L., Mishra, B. & Bernhardt, H.-J. An experimental study on cubanite irreversibility: implications for natural chalcopyrite-cubanite intergrowths. *Euro. J. Mineral.* **11**, 471–476 (1999).
30. Berger, E. L., Keller, L. P. & Lauretta, D. S. An experimental study of the formation of cubanite ($CuFe_2S_3$) in primitive meteorites. *Meteor. Planet. Sci.* **50**, 1–14 (2015).
31. Grossman, J. N., Alexander, C. M. O. D., Wang, J. & Brearley, A. J. Bleached chondrules: evidence for widespread aqueous processes on the parent asteroids of ordinary chondrites. *Meteor. Planet. Sci.* **35**, 467–486 (2000).
32. Keller, L. P. & Berger, E. L. Plagioclase-rich Itokawa grains: Space weathering, exposure ages, and comparison to lunar soil grains. In *Lunar and Planetary Science Conference* 2353 (2017).
33. Noguchi, T. et al. Sylvite and halite on particles recovered from 25143 Itokawa: a preliminary report. *Meteor. Planet. Sci.* **49**, 1305–1314 (2014).
34. Mielczarski, J. A., Cases, J. M., Alnot, M. & Ehrhardt, J. J. XPS characterization of chalcopyrite, tetrahedrite, and tennantite surface products after different conditioning. 1. Aqueous solution at pH 10. *Langmuir* **12**, 2519–2530 (1996).
35. Todd, E. C., Sherman, D. M. & Purton, J. A. Surface oxidation of chalcopyrite ($CuFeS_2$) under ambient atmospheric and aqueous (pH 2-10) conditions: Cu, Fe L- and O K-edge X-ray spectroscopy. *Geochim. Cosmochim. Acta* **67**, 2137–2146 (2003).
36. Rubin, A. E. Metallic copper in ordinary chondrites. *Meteoritics* **29**, 93–98 (1994).
37. Łuszczek, K. & Krzesińska, A. M. Copper in ordinary chondrites: Proxies for resource potential of asteroids and constraints for minimum-invasive and economically efficient exploitation. *Planet. Space Sci.* **194**, 105092 (2020).
38. Vaughan, D. J. & Craig, J. R. in *Geochemistry of Hydrothermal Ore Deposits* (ed. H. L. Barnes) Vol. 8, 367–434 (John Wiley & Sons, 1997).
39. Cabri, L. J. New data on phase relations in the Cu-Fe-S system. *Econ. Geol.* **68**, 443–454 (1973).
40. Ramdohr, P. The opaque minerals in stony meteorites. *J. Geophys. Res.* **68**, 2011–2036 (1963).
41. Leshin, L. A., Rubin, A. E. & McKeegan, K. D. The oxygen isotopic composition of olivine and pyroxene from CI chondrites. *Geochim. Cosmochim. Acta* **61**, 835–845 (1997).
42. Briani, G., Gounelle, M., Bourot-Denise, M. & Zolensky, M. E. Xenoliths and microxenoliths in H chondrites: sampling the zodiacal cloud in the asteroid Main Belt. *Meteor. Planet. Sci.* **47**, 880–902 (2012).
43. Zolensky, M. & Ivanov, A. The Kaidun microbreccia meteorite: a harvest from the inner and outer asteroid belt. *Geochemistry* **63**, 185–246 (2003).
44. Morlok, A. et al. Brecciation and chemical heterogeneities of CI chondrites. *Geochim. Cosmochim. Acta* **70**, 5371–5394 (2006).
45. Blinova, A. I., Zega, T. J., Herd, C. D. K. & Stroud, R. M. Testing variations within the Tagish Lake meteorite—I: mineralogy and petrology of pristine samples. *Meteor. Planet. Sci.* **49**, 473–502 (2014).
46. Yano, H. et al. Touchdown of the Hayabusa Spacecraft at the Muses Sea on Itokawa. *Science* **312**, 1350–1353 (2006).
47. Goh, S. W., Buckley, A. N., Lamb, R. N., Rosenberg, R. A. & Moran, D. The oxidation states of copper and iron in mineral sulfides, and the oxides formed on initial exposure of chalcopyrite and bornite to air. *Geochim. Cosmochim. Acta* **70**, 2210–2228 (2006).
48. Goh, S. W., Buckley, A. N., Skinner, W. M. & Fan, L.-J. An X-ray photoelectron and absorption spectroscopic investigation of the electronic structure of cubanite, $CuFe_2S_3$. *Phys. Chem. Mineral.* **37**, 389–405 (2010).
49. Chen, S.-Y. et al. Electron energy loss spectroscopy and ab initio investigation of iron oxide nanomaterials grown by a hydrothermal process. *Phys. Rev. B* **79**, 104103 (2009).

Acknowledgements

We thank JAXA and the Hayabusa curation team for access to the samples. Funding was provided by NASA LARS awards 80HQTR20T0050 and NNH17AE44I to RMS. We thank our reviewers for providing comments that greatly improved the manuscript.

Author contributions

K.D.B. prepared samples and collected electron microscopy data. R.M.S. provided the samples and guidance on data analysis and interpretation. Both authors contributed to the writing of the manuscript.

Competing interests

The authors declare no competing interests.

Additional information

Supplementary information The online version contains supplementary material available at https://doi.org/10.1038/s43247-021-00187-7.

Correspondence and requests for materials should be addressed to K.D.B.

Peer review information *Communications Earth & Environment* thanks the anonymous reviewers for their contribution to the peer review of this work. Primary handling editors: Mojtaba Fakhraee, Joe Aslin.